

4年给43

ENVIRONMENTAL SCIENCE

ISSN 0250-3301 CODEN HCKHDV HUANJING KEXUE

经济快速发展区场地污染特征、源-汇关系与管控对策专辑

我国经济快速发展区工业VOCs排放特征及管控对策 孟博文,李永波,孟晶,李倩倩,史斌,周喜斌,李金灵,苏贵金



- 主办 中国科学院生态环境研究中心
- ■出版科学出版社





2021年3月

第42卷 第3期 Vol.42 No.3

ENVIRONMENTAL SCIENCE

第42卷 第3期 2021年3月15日

目 次

经济快速发展区场地污染特征、源-汇关系与管控对策专辑
我国经济快速发展区工业 VOCs 排放特征及管控对策 孟博文,李永波,孟晶,李倩倩,史斌,周喜斌,李金灵,苏贵金 (1023)
长江经济带湖北省人为源 VOCs 排放清单及变化特征 ····································
长江经济带湖北省人为源 VOCs 排放清单及变化特征
世 20 年中国表层主壤中多环方烃时至分布特征及源解析
焦化场地内外土壤重金属空间分布及驱动因子差异分析 ····································
要望行化工业项中工粮里金属你胜例及至四万和侯权。
龙岩市某铁锰矿区土壤重金属地球化学空间分布特征与来源分析
基于全周期场地概念模型的场地环境精准调查应用案例 李培中,吴乃瑾,王海见,张骥,荣立明,李翔,魏文侠,宋云(1123)
造纸/ 土壤中短链和中链氯化石蜡的污染特征和风险评估 张佩萱,高丽荣,宋世杰,乔林,徐驰,黄帝,王爽,蒋思静,郑明辉(1131)
典型丹生铜石冰,周边工集中 PCDD/ FS、 PCDS 和 PCNS 的 75条符征及健康/\应广伯
典型再生铜冶炼厂周边土壤中 PCDD/Fs、PCBs 和 PCNs 的污染特征及健康风险评估 胡吉成, 邬静, 许晨阳, 金军 (1141) 柠檬酸与磷共存对土壤吸附镉的影响 宋子腾, 左继超, 胡红青 (1152) 两种能源草田间条件下对镉和锌的吸收累积 郑瑞伦, 石东, 刘文菊, 孙国新, 侯新村, 胡艳霞, 朱毅, 武菊英 (1158)
积特化体早口间采作下对拥和锌的吸收系统
盐胁坦卜八宝景大小同生态型对土壤中 Cd 枳累特仙 · · · · · · · · · · · · · · · · · · ·
水分条件对生物炭钝化水稻土铅镉复合污染的影响
壳聚糖改性生物炭对水稻土甲基汞生成及其稻米积累的影响
铬污染对土壤细菌群落结构及其构建机制的影响····································
研究报告 COVID-19 疫情期间克津冀大气污染物变化及影响因素分析
2020 年初疫情管控对山东省空气质量影响的模拟
南京北郊 PM _{2.5} 中有机组分的吸光性质及来源 ·······················尚玥,余欢,茅宇豪,王成,谢鸣捷(1228)
COVID-19 疫情期间京津冀大气污染物变化及影响因素分析
·····································
1
西宁市大气污染来源和输送季节特征
有句是每个问行采过住下人气积恒心炎解依度分型存证。
 金子上加监例的区三用工业四区周辺人 (拝及)住有机物行架行訊 直接を (1298) 山地型城市冬季大气重污染过程特征及成因分析 一 対作诚、牛月圆、吴婧、闫雨龙、胡冬梅、邱雄辉、彭林 (1306) 一 白城市群主要大气污染物网格化排放清单及来源贡献 一 王文鹏、王占祥、李继祥、高宏、黄韬、毛潇萱、马建民 (1315) 2012 ~ 2019 年北京市储油库 VOCs 去除及排放水平变化监测分析 生活垃圾无害化处理大气污染物排放清单 上 大型、 (1328) 上 大型、 (1328)
山地型城市冬季大气重污染过程特征及成因分析 刘倬诚,牛月圆,吴婧,闫雨龙,胡冬梅,邱雄辉,彭林(1306)
二 日城巾群土安人气行架彻网恰化排放消里及米源贝斯····································
生活垃圾无害化处理大气污染物排放清单 马占云,姜昱聪,任佳雪,张阳,冯鹏,高庆先,孟丹(1333)
长江口邻近海域表层沉积物中的细菌藿多醇及对低氧区的响应判别
鄱阳湖流域水体和水产品甲苯酚的泰露特征及人体健康风险评估 ·
一个一个一个一个一个一个一个一个一个一个一个一个一个一个一个一个一个一个一个
丹江口水库及其入库支流水体中微塑料组成与分布特征 潘雄,林莉,张胜,翟文亮,陶晶祥,李丹文(1372)
金盆水库暴雨径流时空演变过程及水质评价 ·············· 黄诚,黄廷林,李扬,李楠,齐允之,司凡,华逢耀,赵凌云(1380)
汛期暴雨径流对饮用水水库溶解性有机质(DOM)光谱特征的影响 ····································
苏州古城区域河道碳氮磷类污染物的分布特征
娘子关泉群水化学特征及成因 唐春雷,赵春红,申豪勇,梁永平,王志恒(1416)
型氧化钙里型肽沉利水甲瞬酸盐的吸附作用 · · · · · · · · · · · · · · · · · · ·
紫外/亚硫酸盐高级还原工艺加速降解水中难降解含碘造影剂 刘子奇, 仇付国, 赖曼婷, 李津, 董慧峪, 强志民 (1443)
太阳能热活化过硫酸盐降解染料罗丹明 B 的效能
一步法 $La@MgFe_2O_4$ 的制备及其吸附水中磷的性能 ····································
工性风快长块嵌修滤板换生物-纳滤组盲皮爬骨单几仍架物去除双胞 "如立奶,小樱桃,加夜流,口几,早界,凹面丽(1409) ANAMMOX 培养物中硫酸盐型氨氧化生物转化机制 毕贞,董石语,黄勇(1477)
不同季节城市污水处理厂微生物群落特性 贺赟,李魁晓,王佳伟,王慰,樊鹏超,陈行行,王军静(1488)
麻黄碱在斑马鱼体内的器官特异性蓄积及毒代动力学 殷行行,郭昌胜,邓洋慧,邱紫雯,张艳,滕彦国,徐建(1496)
李程遥,黄廷林,温成成,梁伟光,林子深,杨尚业,李凯,蔡晓春(1391)苏州古城区域河道碳氮磷类污染物的分布特征 白冬锐,张涛,陈坦,王洪涛,金曦,郑凯旋,李忠磊,杨婷,金军(1403)娘子关泉群水化学特征及成因 唐春雷,赵春红,申豪勇,梁永平,王志恒(1416)过氧化钙重塑底泥对水中磷酸盐的吸附作用 徐楚天,李大鹏,王子良,吴宇涵,许鑫澎,黄勇(1424)亚热带丘陵区绿狐尾藻人工湿地处理养猪废水氮磷去向 王丽莎,李希,李裕元,张满意,吴金水(1433)紫外/亚硫酸盐高级还原工艺加速降解水中难降解含碘造影剂 刘子奇,仇付国,赖曼婷,李津,董慧峪,强志民(1443)太阳能热活化过硫酸盐降解染料罗丹明 B 的效能 马萌,许路,金鑫,金鹏康(1451)一步法La@MgFe20,的制备及其吸附水中磷的性能 白润英,宋博文,张彧,郝俊峰,刘建明,刘宇红(1461)工程规模长填龄渗滤液膜生物-纳滤组合设施各单元污染物去除效能 邵立明,邓樱桃,仇俊杰,吕凡,章骅,何品晶(1469)ANAMMOX 培养物中硫酸盐型氨氧化生物转化机制 华贞,董石语,黄勇(1477)不同季节城市污水处理厂微生物群落特性 贺崇、李魁晓,王佳伟,王慰,樊鹏超,陈行行,王军静(1488)麻黄碱在斑马鱼体内的器官特异性蓄积及毒代动力学 殷行行,郭昌胜,邓洋慧,邱紫雯,张艳,滕彦国,徐建(1496)内蒙古白云鄂博矿区土壤稀土元素污染特征及评价 王哲,赵莹晨,骆逸飞,郑春丽,卞园,张光宇(1503)广西典型岩溶区农田土壤-作物系统 Cd 迁移富集影响因素
一旦
超顺磁性纳米材料对隔污染稻田土壤微生物和酶的影响
水分管埋与施硅对水稻根表铁膜及砷镉吸收的影响 ····································
地膜覆盖对菜地垄沟 CH. 和 N.O 排放的影响····································
对比研究生物炭和秸秆对麦玉轮作系统 N_2O 排放的影响 ····································
流域水生态空间管控下生境监测方法概述
《环境科学》征订启事(1151) 《环境科学》征稿简则(1342) 信息(1402, 1415, 1580)



长江口邻近海域表层沉积物中的细菌藿多醇及对低氧 区的响应判别

尹美玲^{1,2,3,4}. 段丽琴^{1,2,3,4*}. 宋金明^{1,2,3,4}. 张乃星⁵

(1. 中国科学院海洋研究所海洋生态与环境科学重点实验室,青岛 266071; 2. 中国科学院大学地球与行星科学学院, 北京 100049; 3. 青岛海洋科学与技术国家实验室海洋生态与环境科学功能实验室,青岛 266237; 4. 中国科学院海洋大科 学研究中心,青岛 266071; 5. 国家海洋局北海预报中心,青岛 266033)

摘要:作为新型细菌生物标志物的细菌藿多醇(bacteriohopanepolyols,BHPs)在有机质来源追踪和环境变化响应等方面有明确的指示作用.本文应用高效液相色谱串联大气压化学电离源质谱法(HPLC-APCI-MS)分析,在解析长江口邻近海域表层沉积物中 BHPs 的组成、分布和来源特征基础上,探讨了 BHPs 对长江口邻近海域季节性低氧的指示作用.结果表明,长江口邻近海域表层沉积物中共检测出 12 种 BHPs,其含量范围(以 TOC 计)为 3.79~269 μg·g⁻¹. BHPs 以细菌藿四醇(bacteriohopanetetrol,BHT)、2-甲基 BHT、氨基 BHPs 和腺苷藿烷及同系物为主要组分,分别占总量的40%、22%、12%和4%.各组分含量及相应指标呈现出明显的空间变化趋势,其中,主要来源于海洋自生来源的 BHT 呈现明显的"离岸增加"趋势;主要为陆源贡献的腺苷藿烷等土壤标志物 BHPs 呈现明显的"离岸降低"特征. R_{soil}指数呈现出与腺苷藿烷等土壤标志物 BHPs 相似的空间分布格局,其陆源有机质贡献从近岸的61.5%下降至外海的1.66%,表明长江口邻近海域近岸有机质主要为陆源输入,而外海主要为海源贡献.细菌藿四醇同分异构体 BHT-Ⅱ来源于厌氧氨氧化细菌,其相对含量的高值区与长江口低氧区分布相一致,且与底层水溶解氧(DO)含量呈显著负相关,表明低氧环境有利于 BHT-Ⅱ的生成,BHT-Ⅲ可用于指示海洋低氧区环境特征.

关键词:细菌藿多醇(BHPs);生物地球化学行为;来源判别;低氧;长江口邻近海域中图分类号: X55 文献标识码: A 文章编号: 0250-3301(2021)03-1343-11 **DOI**: 10.13227/j. hjkx. 202007244

Response of Bacteriohopanepolyols to Hypoxic Conditions in the Surface Sediments of the Yangtze Estuary and Its Adjacent Areas

YIN Mei-ling^{1,2,3,4}, DUAN Li-qin^{1,2,3,4}*, SONG Jin-ming^{1,2,3,4}, ZHANG Nai-xing⁵

(1. Key Laboratory of Marine Ecology and Environmental Sciences, Institute of Oceanology, Chinese Academy of Sciences, Qingdao 266071, China; 2. School of Earth and Planetary Sciences, University of Chinese Academy of Sciences, Beijing 100049, China; 3. Laboratory for Marine Ecology and Environmental Sciences, Qingdao National Laboratory for Marine Science and Technology, Qingdao 266237, China; 4. Center for Ocean Mega-Science, Chinese Academy of Sciences, Qingdao 266071, China; 5. North China Sea Marine Forecasting Center of State Oceanic Administration, Qingdao 266033, China)

Abstract: Bacteriohopanepolyols (BHPs), as a novel bacterial biomarker, show clear potential for tracking organic matter sources and environmental change. To evaluate BHPs as indicators of seasonal hypoxia in the Yangtze Estuary and its adjacent areas, the composition, distribution, and source of BHPs in surface sediments were analyzed using high-performance liquid chromatographyatmospheric pressure chemical ionization-mass spectrometry (HPLC-APCI-MS). A total of 12 BHPs were detected with a normalized TOC concentration of 3.79-269 μg·g⁻¹. The BHPs present in the surface sediments were dominated by bacteriohopanetetrol (BHT), 2-methyl-BHT, amino-BHPs, and adenosylhopane and its homologues, accounting for 40%, 22%, 12%, and 4% of the total BHPs, respectively. Each of these components and their corresponding indices show clear spatial trends. Specifically, BHT showed an "offshore increase" trend, which was mainly attributed to marine autochthonous inputs; and soil marker BHPs including adenosylhopane, which were dominated by terrestrial sources, showed an "offshore decrease" trend. The R_{soil} index indicated a similar spatial pattern to the soil marker BHPs, with the relative contribution of terrestrial organic matter decreasing from 61.5% in coastal waters to 1.66% in the open ocean. This suggests that the organic matter in the coastal waters was mainly derived from terrestrial sources while marine sources were dominant in the open ocean. BHT- II, the BHT stereoisomer, was derived from anaerobic ammonium oxidizing bacteria. High BHT-II ratios were consistent with seasonal hypoxic zones in the Yangtze Estuary and, furthermore, these ratios were significantly negatively correlated with dissolved oxygen (DO) concentrations in the bottom waters. These observations indicate that hypoxic environments are beneficial to BHT-II production, implying that BHT-II can be used as an indicator of marine hypoxia.

收稿日期: 2020-07-26; 修订日期: 2020-09-01

基金项目: 国家自然科学基金项目(41976037,41676068); 中国科学院青年促进会项目(2016191); 中国科学院海洋研究所青年汇泉学者项目; 烟台"双百计划"项目

作者简介: 尹美玲(1996~),女,硕士研究生,主要研究方向为海洋生物地球化学,E-mail:yinmeiling18@ mails. ucas. ac. cn

* 通信作者,E-mail;duanliqin@qdio.ac.cn

Key words: bacteriohopanepolyols (BHPs); biogeochemical behavior; origin identification; hypoxia; Yangtze Estuary and its adjacent areas

陆架边缘海的生物地球化学过程和生态环境变化对全球生物要素循环以及海洋生态功能具有重要影响.全球海洋中约有80%以上的沉积有机质埋藏在边缘海碳库,且它们的来源和组成复杂,因而了解和区分边缘海有机质的来源和行为具有重要意义[1,2].同时,由于近年来人类活动和气候变化的影响,海洋低氧现象引起学者的广泛关注.低氧不仅对区域碳氮磷等生源要素的循环过程影响显著,而且会严重破坏海洋生态系统服务功能和生态平衡.我国在20世纪50年代就调查发现长江口海域的季节性低氧,但由于缺乏长期的综合观测以及溶解氧(DO)数据的时限性,对长江口海域低氧状况及其长期变化了解不足[3,4].因而,寻求新的指标来有效指示海洋低氧环境尤为重要.

生物标志化合物由于其来源特异性和环境稳定性,环境指示应用日益广泛^[5,6].最近受到关注的是一种新型微生物标志物——细菌霍多醇(BHPs).BHPs 作为细菌细胞膜的组成成分,其是由多种细菌(包括蓝细菌和固氮细菌等)产生的,五环三萜碳骨架和延伸的官能基团侧链组成的生物藿类物质^[7,8].羟基、氨基和糖基等多种官能团侧链使BHPs 具有结构变异性和种类多样性,而稳定的碳骨架又使BHPs 在沉降和成岩过程中得以保存特定的母源信息.

BHPs 具有细菌来源专属性和环境特异性,可作为生源和环境专属指示指标. 例如研究发现 2-甲基BHPs 主要来源于蓝细菌,可用于指示沉积环境中蓝细菌的微生物量^[9]. Cooke 等^[10]在刚果河流域首次研究发现,腺苷藿烷及其同系物,是一组对土壤微生物具有高度来源专属性的 BHPs,被称为"土壤标志物 BHPs"(soil marker BHPs),可指示陆源有机质向海洋环境的输入、转移和埋藏过程. 35-氨基 BHPs,特别是氨基霍四醇和氨基霍戊醇,对好氧甲烷氧化菌具有来源专属性,被作为"甲烷氧化标志物"广泛应用于追踪环境中的甲烷氧化活动^[11]. 此外,在阿拉伯海和智利沿海等海域均有研究发现,细菌藿四醇(bacteriohopanetetrol,BHT)同分异构体(BHT-II)的含量和分布与低/缺氧环境密切相关,具有作为海洋低氧指标的潜力^[12,13].

BHPs 作为新型微生物标志物,在环境指示方面已表现出明显的应用潜能,但其在中国近海的研究开展很少,环境指示功能尚未明确.本文系统研究了长江口邻近海域表层沉积物中 BHPs 的组成、分布

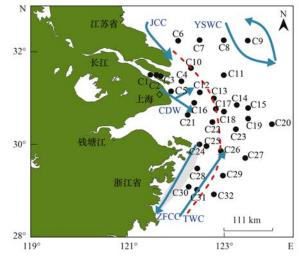
和来源特征,重点探讨了BHPs 在有机质来源判别和低氧环境响应的潜能,旨在揭示BHPs 在长江口邻近海域的环境指示作用,以期为进一步开展BHPs 在其他海洋环境中的指示研究提供理论依据和应用范例.

1 材料与方法

1.1 研究区域与样品采集

长江口邻近海域作为我国主要的边缘海之一,不仅是有机碳的重要碳库,还存在典型的季节性缺氧.长江每年约输送 5×10⁸ t 和 12×10⁶ t 的颗粒物和有机质到长江口近岸海域^[14].长江口低氧区通常于春季形成,低氧面积和程度在夏季达到峰值(可达20 000 km², D0 < 1 mg·L⁻¹),秋季开始减弱至消失^[15].低氧区发生中心和面积存在年际变化,特别是低氧面积和最低含氧量在近 30 年来显著扩大和降低.

于2014年5月在长江口邻近海域利用箱式采样器采集了32个表层沉积物样品(0~2 cm,图1).样晶采集后立即装入高温烧过的铝箔纸袋中于-20℃冷冻保存,带回实验室待用.采用梅特勒 SevenExcellence 多参数分析仪搭配溶解氧电极探头现场测定底层海水溶解氧(DO)浓度,同时采用 Winkler 碘量法对 DO 数据进行校正,相对偏差为±0.03 mg·L⁻¹. 现场样品的采集、保存及环境参数的测定均按照《海洋调查规范》(GB 17378.3-2007)进行.



蓝色箭头表示为水动力系统(CDW:长江冲淡水,ZFCC:浙江-福建 沿岸流,TWC:台湾暖流,JCC:江苏沿岸流,YSWC:黄海暖流), 红色虚线划分近岸和外海海域

图 1 长江口邻近海域表层沉积物采样站位分布示意

Fig. 1 Sampling sites of surface sediments in the Yangtze Estuary and its adjacent areas

1.2 碳与氮的分析

沉积物样品经 2 mol·L⁻¹的盐酸预处理以去除碳酸盐,于 60 °C 烘干至恒重后进行 C、N 元素及同位素分析. 总有机碳(TOC)和总氮(TN)使用 Thermo Flash 2000 元素分析仪测定,相对标准偏差分别为 $\pm 0.02\%$ 和 $\pm 0.002\%$.同位素 δ^{13} C 和 δ^{15} N 使用 Thermo-MAT253 光稳定同位素质谱仪测定,分析误差为 $\pm 0.2\%$.

1.3 BHPs 提取和测定

将沉积物样品冷冻干燥后研磨,称取约 5 g 样品,加入超纯水 (H_2O) /甲醇 (MeOH)/二氯甲烷 (CH_2Cl_2) (4:10:5,体积比)混合试剂,振荡并超声萃取 1 h,离心后取上清液,重复 4 次.将上清液合并加入 $CH_2Cl_2/H_2O(10 \text{ mL},1:1,$ 体积比)后离心,使有机相与水相完全分离.取有机相于氮气下吹干后,加入内标 $(3\alpha,12\alpha\text{-dihydroxy-}5\beta\text{-pregnan-}20\text{-one}3,12\text{-diacetate})$ 、乙酸酐和吡啶 (4 mL,1:1,体积比)于 50℃下乙酰化 1 h,并于室温下放置过夜.乙酰化后的溶液使用氮气吹干后,用 MeOH/异丙醇 (3:2,

体积比)溶解定容,通过高效液相色谱串联大气压 化学电离源质谱(HPLC-APCI-MS)测定 BHPs. 仪器 程序参考 Matys 等[12]的方法:色谱柱流速为 0.19 mL·min⁻¹,温度为 30℃,进样量为 5 μL. 配备有正 离子模式 APCI 源的质谱仪参数设定为:毛细管温 度 155℃, 电压 1200 V, APCI 蒸发器温度 350℃, 电 晕放电电流 4 μA. 流动相采用梯度洗脱,洗脱液 A 为 MeOH/H,O(95:5,体积比)混合试剂,洗脱液 B 为异丙醇. HPLC 流动相梯度如下:100% 洗脱液 A (0~2 min),洗脱液 B 线性增加至 20% (2~20 min),20% B(20~30 min),洗脱液 B 线性增加至 30% (30~40 min),洗脱液 B 线性降低至 0% (40~ 45 min) 并运行 5 min. BHP 的定性判别是基于选择 性离子扫描模式(SIM),扫描分子离子峰为613、 653、655、669、714、761、772、775、788、830、 802、816(表1和图2)和内标(419),结合 MS-MS 模式下的碎裂模式及相对保留时间的比较来确定 的[12,16,17]. BHPs 各组分由其峰面积与内标峰面积对 比获得半定量浓度.

表 1 BHPs 的种类、结构和来源细菌

1 6 /11	Table 1 Nomenclature, structures, and biological sources of BHPs				
名称	英文简称	m/z^{1}	结构式2)	已知来源微生物	
细菌藿四醇	BHT	655ª	1a	蓝细菌、变形杆菌和紫色非硫细菌等多种[7]	
细菌藿四醇同分异构体	ВНТ- Ⅱ	655 a	1a'	厌氧氨氧化菌 ^[18]	
不饱和 BHT	Unsaturated BHT	653ª	3/4a	醋酸菌[7]	
2-甲基 BHT	2-MethylBHT	669 ^a	2a	蓝细菌、沼泽红假单胞菌和变形菌等[9]	
藿四醇酐 /	AnhydroBHT	613 ^b	1 e	未知或成岩产物[19]	
氨基藿三醇	Aminotriol	714^{b}	1 b	甲烷氧化菌等多种[7]	
氨基藿四醇	Aminotetrol	$772^{\rm b}$	$1\mathrm{c}$	甲烷氧化菌[20]和脱硫弧菌[21]	
不饱和氨基藿戊醇	Unsaturated aminopentol	$828^{\rm b}$	3/4d	甲烷氧化菌[20]	
氨基藿戊醇	Aminopentol	$830^{\rm b}$	$1\mathrm{d}$	I型甲烷氧化菌 ^[20]	
氨基藿戊醇同分异构体	Aminopentol isomer	$830^{\rm b}$	$1\mathrm{d}'$	I型甲烷氧化菌 ^[20]	
腺苷藿烷	Adenosylhopane	788 ^b	1f	紫色非硫细菌、氨氧化菌(亚硝化单胞菌)和固氮菌(慢生根瘤菌) ^[7,19]	
2-甲基腺苷藿烷	2-Methyl adenosylhopane	$802^{\rm b}$	2f	固氮菌(慢生根瘤菌)[22]	
腺苷藿烷-Ⅱ	Adenosylhopane-type ${ m I\hspace{1em}I}$	761 ^b	1 g	紫色非硫细菌[22]	
2-甲基腺苷藿烷-Ⅱ	$2\text{-Methyladenosylhopane-type } I\!I$	775 ^b	2g	_	
腺苷藿烷-Ⅲ	${\bf Adenosylhopane\text{-}type} {\rm I\hspace{1em}I\hspace{1em}I}$	$802^{\rm b}$	1 h	_	
2-甲基腺苷藿烷-Ⅲ	$2\text{-Methyladenosylhopane-type} {\rm I\hspace{1em}I\hspace{1em}I}$	816 ^b	2h	_	

1) a 表示 base peak = [M+H-CH₃COOH] +; b 表示 base peak = [M+H] +; 2) 结构式见图 2

1.4 BHPs 指数计算

土壤标志物 BHPs(soil marker BHPs)为陆源来源,包括腺苷藿烷及其同系物^[23]:

土壤标志物 BHPs = 腺苷藿烷 + 2-甲基腺苷藿烷 + 腺苷藿烷-Ⅲ + 2-甲基腺苷藿烷-Ⅲ + 腺苷藿烷-Ⅲ + 2-甲基腺苷藿烷-Ⅲ

(1)

 R_{soil} 指数基于土壤标志物 BHPs 和 BHT 的相对含量计算 $^{[19]}$:

$$R_{\text{soil}} = \frac{\text{soil marker BHPs}}{(\text{soil marker BHPs} + \text{BHT})}$$
 (2)

BHT- II 相对含量基于 BHT- II 与 BHT 计算^[12]:

BHT- II 相对含量 =
$$\frac{BHT-II}{BHT-II + BHT}$$
 (3)

陆源有机质的贡献使用二端元混合模型计算:

$$C = x \cdot C_{\scriptscriptstyle 1} + (1 - x) \cdot C_{\scriptscriptstyle m} \tag{4}$$

式中,x 和 1-x 分别为沉积物中陆源和海源有机质的比例,C、 C_1 和 C_m 分别代表沉积物样品、陆源和海

图 2 BHPs 的结构

Fig. 2 Structures of BHPs

源有机质中 R_{soil} 和 δ^{13} C值.

2 结果与分析

2.1 长江口邻近海域表层沉积物中 BHPs 的分布 特征

长江口邻近海域表层沉积物中共检测到 12 种 BHPs(图 2),包括 BHT(1a,结构式见图 2,下同)、 BHT- I (1a')、2-甲基 BHT(2a)、不饱和 BHT(3/ 4a)、35-氨基 BHPs [氨基藿三醇(1b)、氨基藿四醇 (1c)和氨基藿戊醇(1 d)]、土壤标志物 BHPs [腺苷 藿烷(1f)、腺苷藿烷-Ⅱ(1g)、腺苷藿烷-Ⅲ(1h)、2-甲基腺苷藿烷-Ⅱ(2g)]和藿四醇酐(1e). 表层沉积 物中总 BHPs 含量(以 TOC 计,下同)为 3.79~269 μg·g⁻¹,主要呈现由近岸向外海增加的趋势,其最高 值出现在东北部 C9 站位[图 3(a)]. 包括 BHT、2-甲基 BHT 和不饱和 BHT 在内的四官能化 BHPs 的 含量占总 BHPs 的 80% 以上; 其中 BHT 为最主要组 分,含量为 1.70~80 μg·g⁻¹,平均占总 BHPs 的 40%.BHT含量呈现出向外海显著增加的分布特 征,其在长江口门外具有最低值,为 1.70 µg·g⁻¹; 外海和南部沿海海域含量较高,最高值为80 μg·g⁻¹ 「图 3(b)]. BHT-Ⅱ含量为 0.46~23.63 μg·g⁻¹,占 总 BHPs 的 2.59%~20.19%之间,其在河口和近岸 海域含量较低,最高值出现在31°N 附近的外海海 域(C15) [图 3(c)]. 2-甲基 BHT 的含量为 0.08~ 103 μg·g⁻¹, 平均占比为总 BHPs 的 21. 85%, 其在东 北部上升流区 C9 站位具有最高值[图 3(d)]. 此

外,沉积物样品中检测到4种土壤标志物 BHPs,总 含量为 0.35~6.70 µg·g⁻¹.其中,腺苷藿烷和 2-甲 基腺苷藿烷-Ⅱ含量较高,分别平均占到土壤标志物 BHPs 的 25.56% 和 58.87%. 土壤标志物 BHPs 在长 江口门具有最高值(6.70 μg·g⁻¹),随着离岸距离增 加,其含量呈现出明显的降低趋势[图3(e)].35-氨 基 BHPs 包含四官能(氨基藿三醇)、五官能(氨基藿 四醇)和六官能(氨基藿戊醇)化合物,总含量为 0.18~21.45 μg·g⁻¹. 其中, 氨基藿三醇为 35-氨基 BHPs 中主要成分,其含量为 0.11~19.35 μg·g⁻¹, 平均占到 35-氨基 BHPs 的 80%: 氨基藿四醇和氨 基藿戊醇为检测到的两种甲烷氧化标志物,其含量 分别为 0~2.42 μg·g⁻¹和 0~2.81 μg·g⁻¹,平均占 总 BHPs 的 1.48% 和 1.02%. 甲烷氧化标志物的空 间分布呈现出向外海显著降低的趋势,在长江口及 以南的沿岸区域具有高值[图 3(f)].

2.2 长江口邻近海域表层沉积物中 C、N 及其同位素

长江口邻近海域表层沉积物中的 TOC 和 TN 的含量分别为 $0.13\% \sim 0.78\%$ 和 $0.01\% \sim 0.11\%$,均呈现由河口-近岸海域-外海逐渐降低的趋势. TOC/TN 值为 $6.70 \sim 11.83$,其分布趋势与 TOC 和 TN 一致,也呈现由河口向外海降低的趋势. C 和 N 稳定同位素 δ^{13} C 和 δ^{15} N 值分别为 $-24.90\% \sim -20.44\%$ 和 $3.12\% \sim 8.38\%$,其表现出随离岸距离增加而升高的趋势(图 4).

2.3 长江口邻近海域表层沉积物中 BHPs 的相关指数 表层沉积物中 BHT-II相对含量变化范围为 0.05

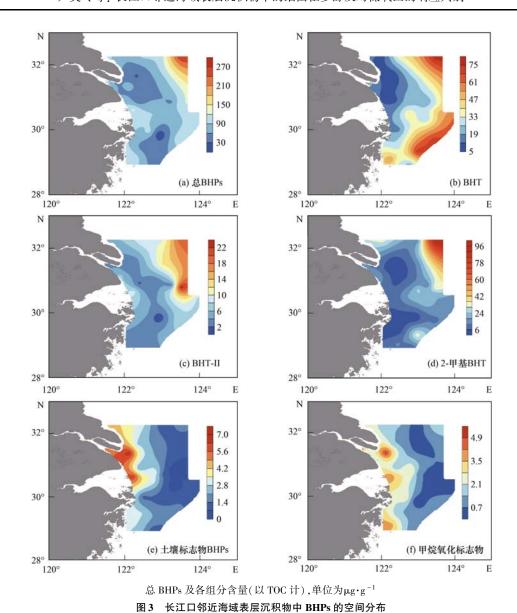


Fig. 3 Spatial distribution of BHPs in surface sediments of the Yangtze Estuary and its adjacent areas

~0.46,平均值为 0.19. BHT-II相对含量的高值区主要分布于北部区域(0.24~0.46),最高值出现在 C6站位,次高值区出现在沿长江冲淡水向外 C15站位(0.42),此外在杭州湾外 C24站位也具有较高值(0.23);低值区出现在长江口门和南部外海海域(图5).表层沉积物中基于 BHPs 的土壤来源指标 R_{soil} 指数变化范围为 0.01~0.40,平均值为 0.10. R_{soil} 指数整体呈现出由河口和近岸海域向外海显著降低的趋势,其最高值出现在长江口门外(图5).

3 讨论

3.1 长江口邻近海域表层沉积物中 BHPs 的陆源来源

3.1.1 土壤标志物 BHPs

土壤标志物 BHPs 及其相关的 R_{soil} 指数已被证实可用来追踪海洋沉积物中 BHPs 的陆源来源 $^{[24,25]}$.有研究发现土壤标志物 BHPs 更容易在土

壤中聚积,其在土壤及有重要陆源输入的河流和近 海沉积物中普遍存在[26]. 因此,海洋沉积物中土壤 标志物 BHPs 通常被认为陆源输入,并通过河流输 送到海洋环境中. 在本研究中, 为判别长江口邻近海 域沉积物中 BHPs 的陆源来源和运移模式,笔者对 比了长江下游地区土壤和长江口邻近海域沉积物中 土壤标志物 BHPs 的含量和分布(图 6). 在长江下 游表层草地类型土壤中,土壤标志物 BHPs 为 BHPs 的主要组分,平均占到总 BHPs 的 30%,与下游河流 沉积物中该组分含量相当. 在长江口邻近海域沉积 物中,土壤标志物 BHPs 的平均质量分数下降为 4.39%,其空间分布呈现出由近岸向外海逐渐降低 的特征,平均相对含量由长江口的 5.87% 逐渐降低 为外海的 1.25%. 土壤标志物 BHPs 这一由土壤向 外海海域显著降低的趋势,表现出其明显的陆源输 入特征. 土壤标志物 BHPs 还呈现出近岸由长江口

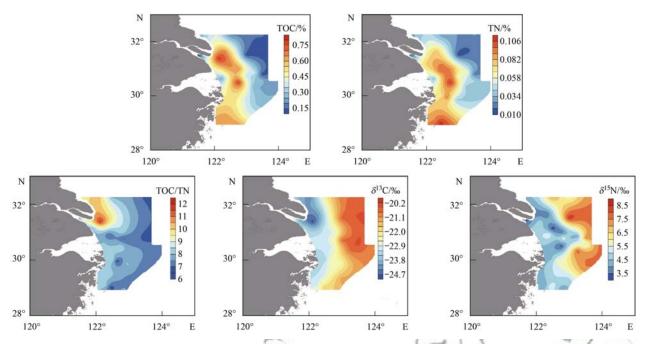


图 4 长江口邻近海域表层沉积物中 TOC、TN、TOC/TN 值、同位素 $\delta^{15}C$ 和 $\delta^{15}N$ 的空间分布

Fig. 4 Spatial distribution of TOC, TN TOC/TN, δ^{13} C, and δ^{15} N in surface sediments of the Yangtze Estuary and its adjacent areas

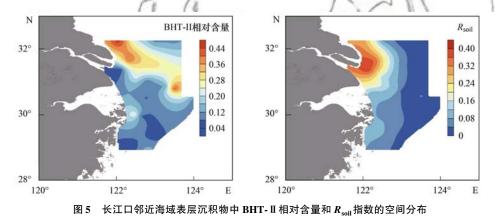


Fig. 5 Spatial distribution of the BHT-II ratios and R_{soil} in surface sediments of the Yangtze Estuary and its adjacent areas

向南逐渐降低的趋势,这主要是土壤中紫色非硫细菌、亚硝化单胞菌和根瘤菌等微生物产生的土壤标志物 BHPs,会附着或结合在大分子有机质上,随长江冲淡水进入长江口,再随浙江福建沿岸流(ZFCC)向南运移的结果^[3,27].长江口北部近岸海域(C6)也呈现出较高含量的土壤标志物 BHPs 值[图 3(e)],这可能是由老黄河口携带的陆源物质随 JCC 沿岸流运移至此的结果.

3.1.2 氨基霍多醇

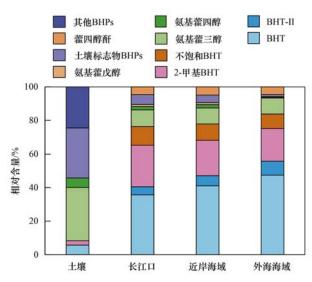
氨基藿三醇由包括甲烷氧化菌在内的多种细菌生成,而氨基霍戊醇和氨基霍四醇分别主要来源于Ⅰ型和Ⅱ型甲烷氧化菌,对甲烷氧化菌具有来源专属性,因此通常将氨基藿四醇、氨基藿戊醇、不饱和氨基藿戊醇和氨基藿戊醇异构体四种组分作为甲烷氧化标志物来指示好氧甲烷氧化活动[11,26].目前,甲烷氧化标志物在陆源和海源系统中均被检测到,

但发现它们在近岸海洋沉积物中的存在归因于陆源湿地来源的有机碳^[24,28]. 在本研究中,长江口邻近海域沉积物中氨基霍四醇和氨基霍戊醇呈现由近岸向外海降低的趋势[图 3(f)],且其与长江流域土壤相比含量显著较低(图 6). 此外,氨基霍四醇和氨基霍戊醇含量与土壤生物标志物 BHPs 含量存在显著正相关(r=0.891,P<0.01; r=0.752, P<0.01). 这些证据均说明氨基霍戊醇和氨基霍四醇可能主要为陆源甲烷氧化菌输入.

3.2 长江口邻近海域表层沉积物中 BHPs 的海源 自生来源

3.2.1 BHT

BHT 在陆地和海洋环境中均存在,其在海洋环境中的含量和分布同时取决于陆源土壤中 BHT 的输入和海洋自生生产. BHT 作为海洋沉积物中BHPs 的最主要成分,其在海洋沉积物中的来源判别



土壤数据来源于文献[19],长江口样品数量 n=5, 近岸海域 n=17,外海海域 n=10

图 6 长江下游土壤和长江口邻近海域表层沉积物中 BHPs 组分的相对含量

Fig. 6 Regionally averaged proportions of individual BHPs in soils and sediments of the Yangtze Estuary and its adjacent areas

对其是否可以作为海洋端元值起着关键作用. 前期 研究发现 BHT 并不是土壤 BHPs 的最主要成分,其 在全球土壤中的含量在4.4%~50%之间,平均值为 15.6%; 而在海洋沉积物中 BHT 为 BHPs 的最主要 成分,约占总 BHPs 的 40%~95%,且呈现向海显著 增加的趋势^[8]. 海洋环境中 BHT 的来源较为广泛 包括蓝细菌(特别是海洋固氮蓝细菌 Crocosphaera sp.)[26],变形杆菌和紫色非硫细菌等多种细 菌[7,21]. 此外,脱硫弧菌属的硫酸盐还原细菌和一些 厌氧氨氧化细菌也是其潜在来源[26].由此可见,海 洋环境中的 BHT 更多为海洋自生产生. 在本研究 中,长江口邻近海域沉积物中 BHT 为 BHPs 的最主 要成分,平均约占 40%,且从近岸的 1.70 μg·g⁻¹ (15%)增加至外海的 80 μg·g⁻¹(61%),这一趋势 表现出其明显的海洋自生来源特征. 此外,长江口邻 近海域沉积物中 BHT 与海洋来源的泉古菌 (Crenarchaeota) 具有显著正相关(r = 0.746, P < 0.01),进一步表明长江口邻近海域表层沉积物中 的 BHT 来源于海洋自生.

3. 2. 2 BHT- II

尽管 BHT-II 的生物来源不确定,但多种证据表明 BHT-II 为海源自生来源,且以厌氧氨氧化细菌为主要来源.目前,BHT-II 尚未在土壤和非海洋厌氧氨氧化菌中检测到[18],说明陆源不是海洋中 BHT-II 的来源.在海洋环境中,BHT-II 仅在海洋厌氧沉积物和海洋最小含氧带中检测到[12],并在海洋厌氧氮氧化菌 Candidatus Scalindua 的培养物中检测

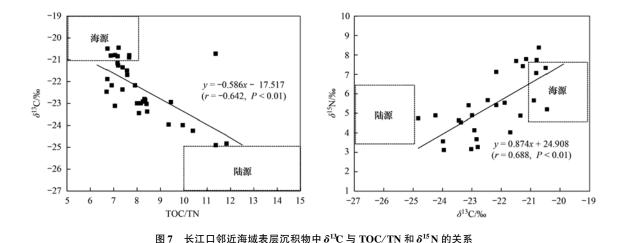
到^[18],而在有氧的大洋环境中未检测到,表明海洋环境中的 BHT- II 主要为低/缺氧环境中的厌氧氨氧化菌生成.在本研究中,长江口邻近海域沉积物中的 BHT- II 呈现显著的向海增加趋势,其由近海的 < 5 μg·g⁻¹增加到外海的 > 15 μg·g⁻¹;且在长江流域土壤和河流沉积物中也未检测到 BHT- II 的存在^[19]. BHT- II 与海洋自生来源的泉古菌含量具有正相关(r=0.522,P<0.01),且其空间分布与由长江口向外海海域显著增加的厌氧氨氧化菌Candidatus Scalindua 基本一致^[29],这些证据均表明长江口邻近海域表层沉积物中的 BHT- II 来源于海洋厌氧氨氧化菌自生.

3.2.3 2-甲基 BHT

2-甲基 BHT 被大量发现于沉积物和实验室培养的蓝细菌中,因此广泛用作蓝细菌的生物标记物^[30]. 在长江口邻近海域沉积物中,2-甲基 BHT 含量分布趋势与 BHT 和 BHT-II 相似,在外海海域呈现高值(>35 μg·g⁻¹). 这与长江口邻近海域中蓝细菌主要活跃在外海海区的分布趋势大致相似^[31],说明长江口邻近海域沉积物中的 2-甲基 BHT 含量分布可能是海洋蓝细菌生产的结果.

3.3 长江口邻近海域表层沉积物中有机质来源分配 海洋沉积物中 TOC/TN 及其稳定同位素 $\delta^{l3}C$ 、 δ¹⁵N 常被用来区分沉积有机质来源海洋藻类还是来 源于陆地植物.已有研究表明,在长江口邻近海域, 由长江携带陆源土壤有机质进入近海的 C/N 比值 为 10~15. 而以浮游植物为主要有机质来源的 C/N 比值为 5~8; δ¹℃ 值在 -21‰~ -19‰之间,其远高 于长江流域陆源有机质中的 δ^{13} C 值(- 27‰~ -25‰)[32]. 在本研究中,长江口邻近海域沉积物中 C/N 比值和 $\delta^{11}C$ 值介于陆源和海源 C/N 比值和 $\delta^{11}C$ 值之间,说明其主要为混合来源(图7),且其空间分 布均说明随离岸距离的增加陆源输入降低,而海源 自生输入显著增加. 为定量评估长江口邻近海域沉 积物中陆源有机质和海洋自生有机质分别所占比 例,笔者采用二元混合模型来计算.分别采用长江流 域陆源和海洋浮游植物中的 δ¹℃ 值为端元值,δ¹³С, 和 δ^{1} \mathbb{C}_{∞} 值分别为 -26% 和 -20%. 通过模型计算得 出长江口邻近海域沉积物中陆源有机质(TOM)和 海源有机质(MOM)所占比例分别为 7.40%~ 81.67% 和 18.33% ~ 92.60%, 平均值分别为 38. 44% 和 61. 56%; 其中陆源有机质呈现向海降低 的趋势,而海源有机质呈现向海增加的趋势(图8).

鉴于 BHPs 稳定的化学结构及组分来源差异,可以根据其陆源组分与海源组分的比值来追踪其陆源输入. R_{soil} 指数也被提出用于估算海洋沉积物中



7 Scatter plots of δ^{13} C and TOC/TN, δ^{15} N in surface sediments of the Yangtze Estuary and its adjacent areas

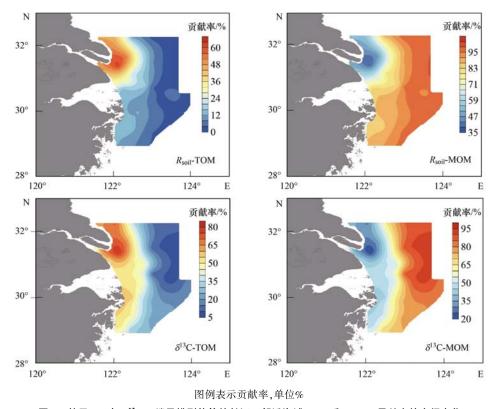


图 8 基于 R_{soil} 与 δ^{13} C 二端元模型估算的长江口邻近海域 TOM 和 MOM 贡献率的空间变化

Fig. 8 Spatial pattern of TOM and MOM contributions based on $R_{\rm soil}$ and δ^{13} C two-terminal models in the Yangtze Estuary and its adjacent areas

BHPs 的陆源与海源配分^[19]. 在上述陆源和海源来源分析中得出长江口邻近海域沉积物中土壤标志物BHPs 和 BHT 分别为陆源输入和海洋自生输入,且BHT 为 BHPs 的最主要组分,因此,基于土壤标志物BHPs 和 BHT 相对含量计算的 R_{soil} 指数适用于本研究中有机质来源判别. 本研究中,长江口邻近海域沉积物中 R_{soil} 指数由长江口门外的 0. 40 迅速降到外海的 0. 01,这一数值和分布趋势与基于 GDGT 的陆源有机质指标 BIT 指数的一致,其从长江口门外的 0. 38 迅速降到外海的 0. 07. 此外, R_{soil} 指数与 δ^{12} C 和 TOC/TN 值之间存在显著相关性 (r = -0.804, P <

0.01;r=0.803,P<0.01,图 9). 这些证据均进一步证明 R_{soil} 在长江口及邻近海域沉积物中陆源有机质来源判别的适用性. 此外,本研究分别选取长江流域土壤中 R_{soil} 的平均值 0.65 和外海海域中 R_{soil} 的平均值 0 作为陆源和海源端元值,运用二端元混合模型,定量计算出河流携带的陆源有机质对长江口邻近海域有机质的贡献为 1.66%~61.54%,其呈现出明显的"离岸降低"特征,特别是在长江口门和北部近岸海域具有高值区(>50%),具有典型的陆源输入特征;而在外海区域下降至<10%(图 8). 这一陆源有机质贡献率及空间变化与 δ^{1} C的二端元模型

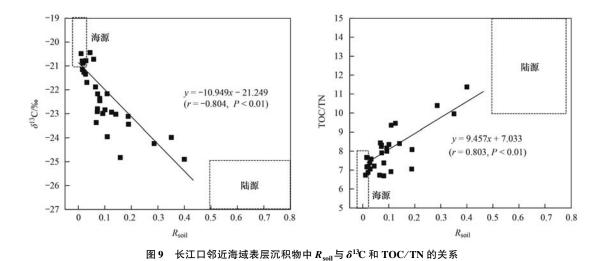


Fig. 9 Scatter plots of R_{soil} and δ^{13} C, TOC/TN ratios in surface sediments of the Yangtze Estuary and its adjacent areas

估算值基本一致,表明长江口邻近海域沉积物有机 质为海陆混合来源;其中,近岸海域主要为陆源有 机质来源,而外海主要为海洋自生来源.

3.4 长江口邻近海域表层沉积物中 BHPs 对低氧的响应

人类活动导致的富营养化与赤潮暴发致使近年来长江口低氧区日益扩大,因此寻求可以指示长江口水体低氧的指示指标至关重要. BHPs 在沉积和转化过程中受到氧化还原条件的影响,对沉积环境的氧化还原状况较为敏感. 在氧化的沉积环境中,BHPs 脱去 C₃₁ ~ C₃₅上的极性基团而被氧化为藿酸和藿醇,然后进一步经脱羧过程和异构化过程形成低碳数的霍烷和藿烯等; 在还原的沉积环境中,高碳数的 BHPs 则倾向于被保留下来^[8],特别是 BHT-II生成于低氧环境,并可稳定保存数百万年^[33]. 因此,可利用沉积物中 BHPs 的特殊组分来指示海洋氧化还原状况.

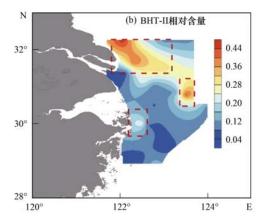
BHT-Ⅱ的水体原位生成和沉积物中的良好保存是沉积物中BHT-Ⅱ作为海水低/缺氧指示指标的

N
32°

DO <2 mg·L⁻¹
DO <3 mg·L⁻¹
DO <3 mg·L⁻¹
DO <3 mg·L⁻¹
2006-08 2007-08
2010-08 2013-08
2010-08 2013-08
2018-07 2020-08

前提. 尽管沉积物中也有厌氧氨氧化菌存在, 也会产 生 BHT- Ⅱ,但长江口邻近海域沉积物中厌氧氨氧化 菌生物量远小于水体中的[34]. 此外,尽管本研究中 并未测定水体中的 BHPs, 但在其它海域研究发现 BHT 和 BHT-Ⅱ 在海洋悬浮颗粒物、沉降颗粒物和 表层沉积物中相对含量较为恒定[13],且沉积物中 BHT-Ⅱ 比值与水体中的比值相当[12]; 这些均说明 表层沉积物中的 BHT-Ⅱ 主要为海洋水体中原位生 成后沉降并保存到沉积物中的. Matys 等[12] 和 Rush 等[33]分别在距今数十万年的海洋沉积物和上新世 腐泥(距今 2.97 Ma)中检测到了 BHT-Ⅱ,证明 BHT-Ⅱ可以稳定保存长达数百万年. 因此, 沉积物 中 BHT- II 可被用来指示水体的氧化还原状况. 在前 期研究中还发现,除 BHT-Ⅱ之外,BHT 也会在最小 含氧带显著增加,因此,Sáenz 等[13] 提出将 BHT-II 相对含量用于 BHT- II 的标准化,并作为低/缺氧环 境的指示指标.

如图 10 所示,在本研究中,通过对照长江口邻 近海域沉积物中 BHT-Ⅱ 相对含量与多年来低氧区



图(a)数据来源于现场测定和文献[4,35],黑色虚线框为本研究区域;图(b)红色虚线框为 BHT-II 相对含量的高值区 图 10 不同年份长江口邻近海域低氧区分布及 BHT-II 相对含量的空间分布

Fig. 10 Spatial distribution of hypoxic areas in different years and BHT-II ratios in the Yangtze Estuary and its adjacent areas

的分布.发现 BHT- Ⅱ 相对含量的 3 个高值区基本均 位于低氧区(DO < 3 mg·L-1)内,其他非低氧区域则 对应较低的 BHT-Ⅱ相对含量值:特别是 BHT-Ⅱ相 对含量在长江口门靠北的高值区与近年来低氧区域 的北移现象更吻合. 利用长江口邻近海域近5年底 层海水 DO 数据与 BHT-Ⅱ 做了统计分析,可以得 出,BHT-Ⅱ比值与 DO 存在显著负相关(r 为 0.556 ~0.820,P < 0.01). 长江口邻近海域沉积物中的 BHT-Ⅱ相对含量高值区与水体中以 Candidatus Scalindua 为代表的厌氧氨氧化菌的高值区也相吻 合[29]. 此外,另一生物标志物梯烷脂已被证明可以 指示厌氧氨氧化活动,其在长江口邻近海域中的高 值区对应于生产力的高值区和溶氧的低值区[35],这 一分布趋势与本研究沉积物中 BHT-Ⅱ 相对含量的 分布基本一致. 综合以上结果,长江口邻近海域沉积 物中的 BHT-Ⅱ主要来源于海洋低氧环境中的厌氧 氨氧化细菌,其相对含量可用于指示底层海水低氧 状况.

4 结论

- (1)长江口邻近海域表层沉积物中共检测出包括细菌藿四醇 BHT、BHT-Ⅱ、土壤标志物 BHPs、2-甲基 BHT 和氨基 BHPs 等主要组分在内的 12 种BHPs. 其中,主要为海洋自生来源的 BHT 呈现明显的"离岸增加"趋势;主要为陆源输入的腺苷藿烷等土壤标志物 BHPs 呈现明显的"离岸降低"特征;2-甲基 BHT 和氨基藿多醇分别主要为海洋蓝细菌和陆源甲烷氧化菌的贡献.
- (2)由土壤标志物 BHPs 和 BHT 相对含量计算的 R_{soil} 指数呈现出向外海显著降低的分布趋势. R_{soil} 和 δ^{I} 它 的二端元混合模型估算均表明长江口邻近海域有机质为海陆混合来源,近岸主要为陆源有机质输入,而外海主要为海洋自生来源.
- (3)BHT-II主要来源于海洋低氧环境中的厌氧 氨氧化细菌,其相对含量的高值区与长江口多年低 氧区分布相一致,且与底层水 DO 含量呈显著负相 关,表明沉积物中的 BHT-II 相对含量可用于指示长 江口邻近海域底层海水低氧状况.

参考文献:

- Berner R A. Burial of organic carbon and pyrite sulfur in the modern ocean; its geochemical and environmental significance
 J]. American Journal of Science, 1982, 282(4): 451-473.
- [2] Carreira R S, Cordeiro L G M S, Bernardes M C, et al. Distribution and characterization of organic matter using lipid biomarkers: a case study in a pristine tropical bay in NE Brazil [J]. Estuarine, Coastal and Shelf Science, 2016, 168: 1-9.
- [3] Duan L Q, Song J M, Liang X M, et al. Dynamics and diagenesis of trace metals in sediments of the Changjiang Estuary

- [J]. Science of the Total Environment, 2019, 675: 247-259.
- [4] Wu Y J, Fan D D, Wang D L, et al. Increasing hypoxia in the Changjiang Estuary during the last three decades deciphered from sedimentary redox-sensitive elements [J]. Marine Geology, 2020, 419, doi: 10.1016/j. margeo. 2019. 106044.
- [5] Duan L Q, Song J M, Yuan H M, et al. Occurrence and origins of biomarker aliphatic hydrocarbons and their indications in surface sediments of the East China Sea [J]. Ecotoxicology and Environmental Safety, 2019, 167: 259-268.
- [6] Song J M. Biogeochemical processes of biogenic elements in China marginal seas[M]. Hangzhou: Zhejiang University Press, 2010
- [7] Cooke M P, Talbot H M, Farrimond P. Bacterial populations recorded in bacteriohopanepolyol distributions in soils from Northern England [J]. Organic Geochemistry, 2008, 39 (9): 1347-1358.
- [8] 尹美玲, 段丽琴, 宋金明, 等. 细菌藿多醇的环境指示作用及其在海洋生态环境重建中的应用[J]. 地质论评, 2020, **66**(6): 1486-1498.

 Yin M L, Duan L Q, Song J M, *et al.* Environmental indication
 - of Bacteriohopanepolyols and its application on eco-environmental reconstruction [J]. Geological Review, 2020, **66** (6): 1486-1498.
- [9] Summons R E, Jahnke L L, Hope J M, et al. 2-Methylhopanoids as biomarkers for cyanobacterial oxygenic photosynthesis [J]. Nature, 1999, 400 (6744): 554-557.
- [10] Cooke M.P., Talbot H.M., Wagner T. Tracking soil organic carbon transport to continental margin sediments using soil-specific hopanoid biomarkers: a case study from the Congo fan (ODP site 1075) [J]. Organic Geochemistry, 2008, 39(8): 965-971.
- [11] Spencer-Jones C L, Wagner T, Dinga B J, et al.

 Bacteriohopanepolyols in tropical soils and sediments from the
 Congo River catchment area [J]. Organic Geochemistry, 2015,
 89-90: 1-13.
- [12] Matys E D, Sepúlveda J, Pantoja S, et al. Bacteriohopanepolyols along redox gradients in the Humboldt Current System off northern Chile[J]. Geobiology, 2017, 15(6): 844-857.
- [13] Sáenz J P, Wakeham S G, Eglinton T I, et al. New constraints on the provenance of hopanoids in the marine geologic record: bacteriohopanepolyols in marine suboxic and anoxic environments [J]. Organic Geochemistry, 2011, 42(11): 1351-1362.
- [14] Duan L Q, Song J M, Yuan H M, et al. The use of sterols combined with isotope analyses as a tool to identify the origin of organic matter in the East China Sea[J]. Ecological Indicators, 2017, 83: 144-157.
- [15] Zhou F, Chai F, Huang D J, et al. Investigation of hypoxia off the Changjiang Estuary using a coupled model of ROMS-CoSiNE [J]. Progress in Oceanography, 2017, 159: 237-254.
- [16] Talbot H M, Watson D F, Murrell J C, et al. Analysis of intact bacteriohopanepolyols from methanotrophic bacteria by reversedphase high-performance liquid chromatography-atmospheric pressure chemical ionisation mass spectrometry [J]. Journal of Chromatography A, 2001, 921(2): 175-185.
- [17] Welander P V, Summons R E. Discovery, taxonomic distribution, and phenotypic characterization of a gene required for 3-methylhopanoid production [J]. Proceedings of the National Academy of Sciences of the United States of America, 2012, 109 (32): 12905-12910.
- [18] Rush D, Damsté J S S, Poulton S W, et al. Anaerobic ammonium-oxidising bacteria: a biological source of the bacteriohopanetetrol stereoisomer in marine sediments [J].

- Geochimica et Cosmochimica Acta, 2014, 140: 50-64.
- [19] Zhu C, Talbot H M, Wagner T, et al. Distribution of hopanoids along a land to sea transect: Implications for microbial ecology and the use of hopanoids in environmental studies[J]. Limnology and Oceanography, 2011, 56(5): 1850-1865.
- [20] Blumenberg M, Seifert R, Michaelis W. Aerobic methanotrophy in the oxic-anoxic transition zone of the Black Sea water column [J]. Organic Geochemistry, 2007, 38(1): 84-91.
- [21] Blumenberg M, Krüger M, Nauhaus K, et al. Biosynthesis of hopanoids by sulfate-reducing bacteria (genus Desulfovibrio) [J]. Environmental Microbiology, 2006, 8(7): 1220-1227.
- [22] Talbot H M, Rohmer M, Farrimond P. Rapid structural elucidation of composite bacterial hopanoids by atmospheric pressure chemical ionisation liquid chromatography/ion trap mass spectrometry[J]. Rapid Communications in Mass Spectrometry, 2007, 21(6): 880-892.
- [23] Rethemeyer J, Schubotz F, Talbot H M, et al. Distribution of polar membrane lipids in permafrost soils and sediments of a small high Arctic catchment [J]. Organic Geochemistry, 2010, 41 (10): 1130-1145.
- [24] De Jonge C, Talbot H M, Bischoff J, et al. Bacteriohopanepolyol distribution in Yenisei River and Kara Sea suspended particulate matter and sediments traces terrigenous organic matter input[J]. Geochimica et Cosmochimica Acta, 2016, 174: 85-101.
- [25] Kim J H, Talbot H M, Zarzycka B, et al. Occurrence and abundance of soil-specific bacterial membrane lipid markers in the Têt watershed (southern France): soil-specific BHPs and branched GDGTs[J]. Geochemistry, Geophysics, Geosystems, 2011, 12(2), doi: 10.1029/2010GC003364.
- [26] Kusch S, Sepulveda J, Wakeham S G. Origin of sedimentary BHPs along a Mississippi River-Gulf of Mexico export transect; insights from spatial and density distributions [J]. Frontiers in Marine Science, 2019, 6, doi: 10.3389/fmars.2019.00729.
- [27] Duan L Q, Song J M, Li X G, et al. Glycerol dialkyl glycerol tetraethers signature in sediments of the East China Sea and its implication on marine and continental climate and environment records[J]. Ecological Indicators, 2019, 103: 509-519.
- [28] Wagner T, Kallweit W, Talbot H M, et al. Microbial biomarkers

- support organic carbon transport from methane-rich Amazon wetlands to the shelf and deep sea fan during recent and glacial climate conditions [J]. Organic Geochemistry, 2014, 67: 85-98.
- [29] 姜晓芬. 河口近岸厌氧氨氧化菌群结构、丰度及活性对盐度变化的响应[D]. 上海: 华东师范大学, 2017.

 Jiang X F. Responses of anammox bacterial community structure, abundance, and activity to salinity changes in estuarine and coastal sediments[D]. Shanghai: East China Normal University, 2017.
- [30] Blumenberg M, Arp G, Reitner J, et al. Bacteriohopanepolyols in a stratified cyanobacterial mat from Kiritimati (Christmas Island, Kiribati) [J]. Organic Geochemistry, 2013, 55: 55-62
- [31] 丁昌玲, 孙军, 周峰. 东海低氧区及邻近海域固氮蓝藻丰度与分布[J]. 海洋湖沼通报, 2012, (4): 177-188.

 Ding C L, Sun J, Zhou F. The quantities and distributions of nitrogen-fixing cyanobacteria along hypoxia area and adjacent waters in the East China Sea[J]. Transactions of Oceanology and Limnology, 2012, (4): 177-188.
- [32] Zhang J, Wu Y, Jennerjahn T C, et al. Distribution of organic matter in the Changjiang (Yangtze River) Estuary and their stable carbon and nitrogen isotopic ratios: implications for source discrimination and sedimentary dynamics[J]. Marine Chemistry, 2007, 106(1-2): 111-126.
- [33] Rush D, Damsté J S S. Lipids as paleomarkers to constrain the marine nitrogen cycle [J]. Environmental Microbiology, 2017, 19(6): 2119-2132.
- [34] 吴冬梅. 长江口和东海海域细菌群落结构及其生态功能预测 [D]. 舟山; 浙江海洋大学, 2018.
 Wu D M. Composition and predictive functional analysis of bacterial communities in the Changjiang Estuary and the East China Sea[D]. Zhoushan; Zhejiang Ocean University, 2018.
- [35] 曹亚俐. 利用生物标志物梯烷脂研究东海厌氧氨氧化活动的 时空分布特征[D]. 青岛: 中国海洋大学, 2013. Cao Y L. The study on the spatial and temporal distributions of anammox in the East China Sea by ladderane lipids [D]. Qingdao; Ocean University of China, 2013.

HUANJING KEXUE

Environmental Science (monthly)

Vol. 42 No. 3 Mar. 15, 2021

CONTENTS

CONTENTS	
Industrial Emission Characteristics and Control Countermeasures of VOCs in Chinese Rapid Economic Development Areas	
VOCs Emission Inventory and Variation Characteristics of Artificial Sources in Hubei Province in the Yangtze River Economic Belt	
Sources and Distribution Characteristics of HCBD in Rapid Economic Development Areas	
Polycyclic Aromatic Hydrocarbons in Surface Soil of China (2000-2020); Temporal and Spatial Distribution, Influencing Factors	
Relationships Between Microplastic and Surrounding Soil in an E-Waste Zone of China	······ CHAI Bing-wen, YIN Hua, WEI Qiang, et al. (1073)
Analysis of the Spatial Distribution of Heavy Metals in Soil from a Coking Plant and Its Driving Factors	·· GU Gao-quan, WAN Xiao-ming, ZENG Wei-bin, et al. (1081)
Source Apportionment and Spatial Distribution Simulation of Heavy Metals in a Typical Petrochemical Industrial City	····· SUN Xue-fei, ZHANG Li-xia, DONG Yu-long, et al. (1093)
Heavy Metal Contents of Soil and Surface Dust and Its Ecological Risk Analysis in a Multifunctional Industrial Park	·· ZENG Wei-bin, GU Gao-quan, WAN Xiao-ming, et al. (1105)
Geochemical Patterns and Source Analysis of Soil Heavy Metals in an Iron and Manganese Ore Area of Longyan City	
Application Case of Accurate Site Investigation with Life-Cycle Conceptual Site Model Development	
Levels and Risk Assessment of Short and Medium-Chain Chlorinated Paraffins in Soil from Paper Mill Area	
Characterization and Health Risks of PCDD/Fs, PCBs, and PCNs in the Soil Around a Typical Secondary Copper Smelter	
Effect of Citric Acid and Phosphorus Coexistence on Cadmium Adsorption by Soil	
Uptake and Accumulation of Cadmium and Zinc by Two Energy Grasses: A Field Experiment	
Bioaccumulation and Translocation Characteristics of Heavy Metals in a Soil-Maize System in Reclaimed Land and Surrounding Areas	s of Typical Vanadium-Titanium Magnetite Tailings
, , , , , , , , , , , , , , , , , , , ,	
Cd Accumulation Characteristics in Different Populations of Hylotelephium spectabile Under Salt Stress	
Effect of Water Regimes on Pb and Cd Immobilization by Biochar in Contaminated Paddy Soil	
Effects of Chitosan-modified Biochar on Formation of Methylmercury in Paddy Soils and Its Accumulation in Rice	
Effects of Chromium Pollution on Soil Bacterial Community Structure and Assembly Processes	YU Hao, AN Yi-jun, JIN De-cai, et al. (1197)
Analysis of Changes and Factors Influencing Air Pollutants in the Beijing-Tianjin-Hebei Region During the COVID-19 Pandemic …	······· ZHAO Xue, SHEN Nan-chi, LI Ling-jun, et al. (1205)
Impact of Pollutant Emission Reduction on Air Quality During the COVID-19 Pandemic Control in Early 2020 Based on RAMS-CMA	
Light-absorbing Properties and Sources of PM _{2, 5} Organic Components at a Suburban Site in Northern Nanjing	
Pollution Characteristics and Chromophore Types of Brown Carbon in Xi'an	
Source and Health Risk Assessment of PM _{2,5} -Bound Metallic Elements in Road Dust in Zibo City	
Health Benefit Assessment of PM _{2, 5} Pollution Control in Beijing	
Seasonal Characteristics of Air Pollutant Sources and Transport Pathways in Xining City	
Concentrations and Patterns of Atmospheric Particulate Nitrogen and Phosphorus During Different Weather Conditions in Qingdao Coa	
Characterization of Volatile Organic Compounds (VOCs) Using Mobile Monitoring Around the Industrial Parks in the Yangzte River	
(100)	····· WANG Hong-li GAO Ya-qin IING Sheng-ao et al. (1298)
Characteristics and Cause Analysis of Heavy Air Pollution in a Mountainous City During Winter	
Gridded Emission Inventories of Major Criteria Air Pollutants and Source Contributions in Lan-Bai Metropolitan Area, Northwest Chin	
	WANG Wen-peng, WANG Zhan-xiang, LI Ji-xiang, et al. (1315)
VOCs Removal and Emission Monitoring of Beijing Bulk Gasoline Terminals in 2012-2019	
Emission Inventory of Air pollutants for the Harmless Treatment of Municipal Solid Waste	
Response of Bacteriohopanepolyols to Hypoxic Conditions in the Surface Sediments of the Yangtze Estuary and Its Adjacent Areas	
Human Health Risk Assessment of Phenol in Poyang Lake Basin	
Spatial-Temporal Variation of Water Environment Quality and Pollution Source Analysis in Hengshui Lake	
Composition and Distribution Characteristics of Microplastics in Danjiangkou Reservoir and Its Tributaries	
Temporal and Spatial Evolution of Storm Runoff and Water Quality Assessment in Jinpen Reservoir	
Influence of Storm Runoff on the Spectral Characteristics of Dissolved Organic Matter (DOM) in a Drinking Water Reservoir During	
inituence of Storm Runoit on the Spectral Characteristics of Dissolved Organic Matter (DOM) in a Drinking Water Reservoir During	I Change I HIANG Tankin WEN Changlang April (1201)
Distribution Characteristics of Carbon, Nitrogen, and Phosphorus Bearing Pollutants in the Ancient Town Rivers of Suzhou	
Chemical Characteristics and Causes of Groups Water in Niangziguan Spring	
Adsorption Behavior of Phosphate by CaO ₂ Remolded Sediment	
Nitrogen and Phosphorus Removal in Surface Flow Constructed Wetland Planted with Myriophyllum elatinoides Treating Swine Waster	water in Subtropical Central China
Accelerated Degradation of Aqueous Recalcitrant Iodinated Contrasting Media Using a UV/SO ₃ ² - Advanced Reduction Process ····	
Degradation of Dye Rhodamine B by Solar Thermally Activated Persulfate	
Degradation of Dye Rhodamine B by Solar Thermally Activated Persulfate One-step Preparation of Lanthanum-Magnesium Ferrite and Its Phosphate Adsorption Capacity in Aqueous Solutions	
One-step Preparation of Lanthanum-Magnesium Ferrite and Its Phosphate Adsorption Capacity in Aqueous Solutions Pollutant Removal Efficiency of Different Units Along a Mature Landfill Leachate Treatment Process in a Membrane Biological React	BAI Run-ying, SONG Bo-wen, ZHANG Yu, et al. (1461) or-Nanofiltration Combined Facility
One-step Preparation of Lanthanum-Magnesium Ferrite and Its Phosphate Adsorption Capacity in Aqueous Solutions Pollutant Removal Efficiency of Different Units Along a Mature Landfill Leachate Treatment Process in a Membrane Biological Reaction	BAI Run-ying, SONG Bo-wen, ZHANG Yu, et al. (1461) or-Nanofiltration Combined Facility
One-step Preparation of Lanthanum-Magnesium Ferrite and Its Phosphate Adsorption Capacity in Aqueous Solutions Pollutant Removal Efficiency of Different Units Along a Mature Landfill Leachate Treatment Process in a Membrane Biological Reacted Solutions Biological Conversion Mechanism of Sulfate Reduction Ammonium Oxidation in ANAMMOX Consortia	BAI Run-ying, SONG Bo-wen, ZHANG Yu, et al. (1461) or-Nanofiltration Combined Facility
One-step Preparation of Lanthanum-Magnesium Ferrite and Its Phosphate Adsorption Capacity in Aqueous Solutions Pollutant Removal Efficiency of Different Units Along a Mature Landfill Leachate Treatment Process in a Membrane Biological Reacter Biological Conversion Mechanism of Sulfate Reduction Ammonium Oxidation in ANAMMOX Consortia Microbial Community Structure of Waste Water Treatment Plants in Different Seasons	or-Nanofiltration Combined Facility
One-step Preparation of Lanthanum-Magnesium Ferrite and Its Phosphate Adsorption Capacity in Aqueous Solutions Pollutant Removal Efficiency of Different Units Along a Mature Landfill Leachate Treatment Process in a Membrane Biological Reaction	or-Nanofiltration Combined Facility
One-step Preparation of Lanthanum-Magnesium Ferrite and Its Phosphate Adsorption Capacity in Aqueous Solutions Pollutant Removal Efficiency of Different Units Along a Mature Landfill Leachate Treatment Process in a Membrane Biological React Biological Conversion Mechanism of Sulfate Reduction Ammonium Oxidation in ANAMMOX Consortia Microbial Community Structure of Waste Water Treatment Plants in Different Seasons Organ-Specific Accumulation and Toxicokinetics of Ephedrine in Adult Zebrafish (Danio rerio) Y Characteristics and Evaluation of Soil Rare Earth Element Pollution in the Bayan Obo Mining Region of Inner Mongolia	BAI Run-ying, SONG Bo-wen, ZHANG Yu, et al. (1461) or-Nanofiltration Combined Facility
One-step Preparation of Lanthanum-Magnesium Ferrite and Its Phosphate Adsorption Capacity in Aqueous Solutions Pollutant Removal Efficiency of Different Units Along a Mature Landfill Leachate Treatment Process in a Membrane Biological Reacter Science Sc	BAI Run-ying, SONG Bo-wen, ZHANG Yu, et al. (1461) or-Nanofiltration Combined Facility
One-step Preparation of Lanthanum-Magnesium Ferrite and Its Phosphate Adsorption Capacity in Aqueous Solutions Pollutant Removal Efficiency of Different Units Along a Mature Landfill Leachate Treatment Process in a Membrane Biological React Biological Conversion Mechanism of Sulfate Reduction Ammonium Oxidation in ANAMMOX Consortia Microbial Community Structure of Waste Water Treatment Plants in Different Seasons Organ-Specific Accumulation and Toxicokinetics of Ephedrine in Adult Zebrafish (Danio rerio) Y Characteristics and Evaluation of Soil Rare Earth Element Pollution in the Bayan Obo Mining Region of Inner Mongolia	BAI Run-ying, SONG Bo-wen, ZHANG Yu, et al. (1461) or-Nanofiltration Combined Facility
One-step Preparation of Lanthanum-Magnesium Ferrite and Its Phosphate Adsorption Capacity in Aqueous Solutions Pollutant Removal Efficiency of Different Units Along a Mature Landfill Leachate Treatment Process in a Membrane Biological Reacter Biological Conversion Mechanism of Sulfate Reduction Ammonium Oxidation in ANAMMOX Consortia Microbial Community Structure of Waste Water Treatment Plants in Different Seasons Organ-Specific Accumulation and Toxicokinetics of Ephedrine in Adult Zebrafish (Danio rerio) Y Characteristics and Evaluation of Soil Rare Earth Element Pollution in the Bayan Obo Mining Region of Inner Mongolia Factors Affecting the Translocation and Accumulation of Cadmium in a Soil-Crop System in a Typical Karst Area of Guangxi Province Effects of Superparamagnetic Nanomaterials on Soil Microorganisms and Enzymes in Cadmium-Contaminated Paddy Fields	BAI Run-ying, SONG Bo-wen, ZHANG Yu, et al. (1461) or-Nanofiltration Combined Facility
One-step Preparation of Lanthanum-Magnesium Ferrite and Its Phosphate Adsorption Capacity in Aqueous Solutions Pollutant Removal Efficiency of Different Units Along a Mature Landfill Leachate Treatment Process in a Membrane Biological Reacter Solution Ammonium Oxidation in ANAMMOX Consortia Microbial Community Structure of Waste Water Treatment Plants in Different Seasons Organ-Specific Accumulation and Toxicokinetics of Ephedrine in Adult Zebrafish (Danio rerio) Y Characteristics and Evaluation of Soil Rare Earth Element Pollution in the Bayan Obo Mining Region of Inner Mongolia Factors Affecting the Translocation and Accumulation of Cadmium in a Soil-Crop System in a Typical Karst Area of Guangxi Province Effects of Superparamagnetic Nanomaterials on Soil Microorganisms and Enzymes in Cadmium-Contaminated Paddy Fields Effects of Water Management and Silicon Application on Iron Plaque Formation and Uptake of Arsenic and Cadmium by Rice	BAI Run-ying, SONG Bo-wen, ZHANG Yu, et al. (1461) or-Nanofiltration Combined Facility
One-step Preparation of Lanthanum-Magnesium Ferrite and Its Phosphate Adsorption Capacity in Aqueous Solutions Pollutant Removal Efficiency of Different Units Along a Mature Landfill Leachate Treatment Process in a Membrane Biological Reacter. Biological Conversion Mechanism of Sulfate Reduction Ammonium Oxidation in ANAMMOX Consortia Microbial Community Structure of Waste Water Treatment Plants in Different Seasons Organ-Specific Accumulation and Toxicokinetics of Ephedrine in Adult Zebrafish (Danio rerio) Y Characteristics and Evaluation of Soil Rare Earth Element Pollution in the Bayan Obo Mining Region of Inner Mongolia Factors Affecting the Translocation and Accumulation of Cadmium in a Soil-Crop System in a Typical Karst Area of Guangxi Province Effects of Superparamagnetic Nanomaterials on Soil Microorganisms and Enzymes in Cadmium-Contaminated Paddy Fields	BAI Run-ying, SONG Bo-wen, ZHANG Yu, et al. (1461) or-Nanofiltration Combined Facility
One-step Preparation of Lanthanum-Magnesium Ferrite and Its Phosphate Adsorption Capacity in Aqueous Solutions Pollutant Removal Efficiency of Different Units Along a Mature Landfill Leachate Treatment Process in a Membrane Biological Reacter. Biological Conversion Mechanism of Sulfate Reduction Ammonium Oxidation in ANAMMOX Consortia Microbial Community Structure of Waste Water Treatment Plants in Different Seasons Organ-Specific Accumulation and Toxicokinetics of Ephedrine in Adult Zebrafish (Danio rerio) Y Characteristics and Evaluation of Soil Rare Earth Element Pollution in the Bayan Obo Mining Region of Inner Mongolia Factors Affecting the Translocation and Accumulation of Cadmium in a Soil-Crop System in a Typical Karst Area of Guangxi Province Effects of Superparamagnetic Nanomaterials on Soil Microorganisms and Enzymes in Cadmium-Contaminated Paddy Fields Effects of Water Management and Silicon Application on Iron Plaque Formation and Uptake of Arsenic and Cadmium by Rice Biological Effect of Tetracycline Antibiotics on a Soil-Lettuce System and Its Migration Degradation Characteristics Effect of Plastic Film Mulching on Methane and Nitrous Oxide Emissions from the Ridges and Furrows of a Vegetable Field	BAI Run-ying, SONG Bo-wen, ZHANG Yu, et al. (1461) or-Nanofiltration Combined Facility
One-step Preparation of Lanthanum-Magnesium Ferrite and Its Phosphate Adsorption Capacity in Aqueous Solutions Pollutant Removal Efficiency of Different Units Along a Mature Landfill Leachate Treatment Process in a Membrane Biological Reacter. Biological Conversion Mechanism of Sulfate Reduction Ammonium Oxidation in ANAMMOX Consortia Microbial Community Structure of Waste Water Treatment Plants in Different Seasons Organ-Specific Accumulation and Toxicokinetics of Ephedrine in Adult Zebrafish (Danio rerio) Y Characteristics and Evaluation of Soil Rare Earth Element Pollution in the Bayan Obo Mining Region of Inner Mongolia Factors Affecting the Translocation and Accumulation of Cadmium in a Soil-Crop System in a Typical Karst Area of Guangxi Province Effects of Superparamagnetic Nanomaterials on Soil Microorganisms and Enzymes in Cadmium-Contaminated Paddy Fields Effects of Water Management and Silicon Application on Iron Plaque Formation and Uptake of Arsenic and Cadmium by Rice Biological Effect of Tetracycline Antibiotics on a Soil-Lettuce System and Its Migration Degradation Characteristics Effect of Plastic Film Mulching on Methane and Nitrous Oxide Emissions from the Ridges and Furrows of a Vegetable Field	BAI Run-ying, SONG Bo-wen, ZHANG Yu, et al. (1461) or-Nanofiltration Combined Facility
One-step Preparation of Lanthanum-Magnesium Ferrite and Its Phosphate Adsorption Capacity in Aqueous Solutions Pollutant Removal Efficiency of Different Units Along a Mature Landfill Leachate Treatment Process in a Membrane Biological Reacter and Cadmium of Sulfate Reduction Ammonium Oxidation in ANAMMOX Consortia Biological Conversion Mechanism of Sulfate Reduction Ammonium Oxidation in ANAMMOX Consortia Microbial Community Structure of Waste Water Treatment Plants in Different Seasons Organ-Specific Accumulation and Toxicokinetics of Ephedrine in Adult Zebrafish (Danio rerio) Y Characteristics and Evaluation of Soil Rare Earth Element Pollution in the Bayan Obo Mining Region of Inner Mongolia Factors Affecting the Translocation and Accumulation of Cadmium in a Soil-Crop System in a Typical Karst Area of Guangxi Province Effects of Superparamagnetic Nanomaterials on Soil Microorganisms and Enzymes in Cadmium-Contaminated Paddy Fields Effects of Water Management and Silicon Application on Iron Plaque Formation and Uptake of Arsenic and Cadmium by Rice Biological Effect of Tetracycline Antibiotics on a Soil-Lettuce System and Its Migration Degradation Characteristics Effect of Plastic Film Mulching on Methane and Nitrous Oxide Emissions from the Ridges and Furrows of a Vegetable Field XION	BAI Run-ying, SONG Bo-wen, ZHANG Yu, et al. (1461) or-Nanofiltration Combined Facility
One-step Preparation of Lanthanum-Magnesium Ferrite and Its Phosphate Adsorption Capacity in Aqueous Solutions Pollutant Removal Efficiency of Different Units Along a Mature Landfill Leachate Treatment Process in a Membrane Biological Reacter. Biological Conversion Mechanism of Sulfate Reduction Ammonium Oxidation in ANAMMOX Consortia Microbial Community Structure of Waste Water Treatment Plants in Different Seasons Organ-Specific Accumulation and Toxicokinetics of Ephedrine in Adult Zebrafish (Danio rerio) Y Characteristics and Evaluation of Soil Rare Earth Element Pollution in the Bayan Obo Mining Region of Inner Mongolia Factors Affecting the Translocation and Accumulation of Cadmium in a Soil-Crop System in a Typical Karst Area of Guangxi Province Effects of Superparamagnetic Nanomaterials on Soil Microorganisms and Enzymes in Cadmium-Contaminated Paddy Fields Effects of Water Management and Silicon Application on Iron Plaque Formation and Uptake of Arsenic and Cadmium by Rice Biological Effect of Tetracycline Antibiotics on a Soil-Lettuce System and Its Migration Degradation Characteristics Effect of Plastic Film Mulching on Methane and Nitrous Oxide Emissions from the Ridges and Furrows of a Vegetable Field	BAI Run-ying, SONG Bo-wen, ZHANG Yu, et al. (1461) or-Nanofiltration Combined Facility